

Histone deacetylase inhibition sensitizes p53-deficient B-cell precursor acute lymphoblastic leukemia to chemotherapy

Willem P.J. Cox,¹ Nils Evander,¹ Dorette S. van Ingen Schenau,¹ Gawin R. Stoll,¹ Nadia Anderson,¹ Lieke de Groot,¹ Kari J.T. Grünwald,¹ Rico Hagelaar,^{1,2} Miriam Butler,¹ Roland P. Kuiper,^{1,3} Laurens T. van der Meer^{1#} and Frank N. van Leeuwen^{1#}

¹Princess Máxima Center for Pediatric Oncology and ²Oncode Institute and ³Department of Genetics, Utrecht University Medical Center, Utrecht University, Utrecht, the Netherlands

[#]LTvdM and FNvL contributed equally as senior authors.

Correspondence: F.N. van Leeuwen
f.n.vanleeuwen@prinsesmaximacentrum.nl


Received: August 17, 2023.

Accepted: December 13, 2023.

Early view: December 21, 2023.

<https://doi.org/10.3324/haematol.2023.284101>

©2024 Ferrata Storti Foundation

Published under a CC BY-NC license 

Abstract

In pediatric acute lymphoblastic leukemia (ALL), mutations/deletions affecting the *TP53* gene are rare at diagnosis. However, at relapse about 12% of patients show *TP53* aberrations, which are predictive of a very poor outcome. Since p53-mediated apoptosis is an endpoint for many cytotoxic drugs, loss of p53 function frequently leads to therapy failure. In this study we show that CRISPR/Cas9-induced loss of *TP53* drives resistance to a large majority of drugs used to treat relapsed ALL, including novel agents such as inotuzumab ozogamicin. Using a high-throughput drug screen, we identified the histone deacetylase inhibitor romidepsin as a potent sensitizer of drug responsiveness, improving sensitivity to all chemotherapies tested. In addition, romidepsin improved the response to cytarabine in *TP53*-deleted ALL cells *in vivo*. Together, these results indicate that the histone deacetylase inhibitor romidepsin can improve the efficacy of salvage therapies for relapsed *TP53*-mutated leukemia. Since romidepsin has been approved for clinical use in some adult malignancies, these findings may be rapidly translated to clinical practice.

Introduction

With an overall survival rate that exceeds 90%, pediatric acute lymphoblastic leukemia (ALL) has one of the best outcomes among all pediatric cancers.¹ However, relapsed ALL remains a significant clinical problem. Aberrations affecting the *TP53* gene, although not very common at diagnosis with an incidence of less than 3%, are associated with a dismal prognosis in relapsed ALL in both children and adults in whom the incidences are 12% and 35%, respectively.²⁻⁴ Consequently, relapsed *TP53*-deleted ALL is now classified as ‘very high risk’ in children. Most often the function of both *TP53* alleles is affected, either through direct perturbation of the allele or through dominant-negative effects of one mutated allele over the remaining allele. The encoded p53 protein acts as a transcription factor that coordinates responses to a variety of cellular stressors by controlling the expression of genes involved in cell cycle regulation, apoptosis, and metabolism.⁵ Importantly, p53-mediated apoptosis is an endpoint for many anti-cancer agents. Loss of p53 functions consequently

induces failure not only of classical chemotherapeutics but also of many newly introduced treatments. Hence, there is a continued need for the identification of drugs or drug combinations that effectively eradicate *TP53*-mutated leukemic cells. In this study, we modeled *TP53* deletions in B-cell precursor (BCP)-ALL cell lines and exposed these models to the armamentarium used in the treatment of relapsed ALL. Moreover, we performed a high-throughput drug screen to identify targeted agents that could be used to restore response to current (chemo)therapies.

Methods

Information on model generation, reagents, primers, plasmids, and antibodies can be found in the *Online Supplementary Material*.

Cell viability assays

Cells were seeded at 0.5×10^6 cells/mL in 96-well plates and

cultured in the presence of test compounds for 72 hours. Viability was assessed by measuring membrane integrity or metabolic activity. Membrane integrity was measured by flow cytometry using amine staining (LIVE/DEAD™ Fixable Far-Red Dead Cell Stain Kit, L34974; Thermo Fisher Scientific) and metabolic activity was measured by 3-(4,5-dimethylthiazol-2-yl)-2,5-diphenyltetrazolium bromide (MTT, 475989; Sigma-Aldrich) conversion as the cell readout, both according to the manufacturers' instructions. *Ex vivo* co-culture was performed as described previously.⁶ For drug screening, 0.4x10⁶ cells/mL were seeded in 384-well plates using a multidrop combi reagent dispenser (Thermo Scientific). In a fully automated system, drugs, dissolved in dimethylsulfoxide or water, were added shortly after seeding of the cells with a Biomek i7 liquid handler at the high-throughput screening facility of Princess Máxima Center. An Echo550 dispenser was used for direct drug transfers. MTT conversion was used as the cell readout according to the manufacturer's protocol and area under the curve (AUC) values were calculated. For further downstream analysis, AUC values of p53-knockout (p53^{KO}) cells were normalized for the wild-type (p53^{WT}) cells per drug within each cell line.

Western blotting

Proteins were extracted from cells with Laemmli buffer and boiled. Lysates from equal numbers of cells were separated by sodium dodecylsulfate polyacrylamide gel electrophoresis and subsequently transferred to a polyvinylidene fluoride membrane. Blocking and staining conditions are described in *Online Supplementary Table S1*. Proteins were visualized with the Odyssey® CLx and accompanying Image Studio software (LI-COR Biotechnology).

RNA sequencing

Cells were treated for 16 hours with 2 nM romidepsin, 200 nM cytarabine, or a combination thereof (11 conditions in triplicate, 4 in duplicate, 1 in quadruplicate). mRNA was purified from cell cultures using a NucleoSpin RNA isolation kit (740955, Machery-Nagel). RNA sequencing and data processing on samples were conducted by NovoGene (Cambridge, UK). Gene set enrichment analysis (GSEA) was performed on all genes with sum of fragments per kilobase million (FPKM) values greater than three per cell line for published gene sets in the Molecular Signatures Database (MSigDB).⁷⁻⁹ Differential gene expressions were filtered by *P* value (excluded *P* values <0.05) and fold changes (excluded log₂ values between -0.5 and 0.5) prior to further analysis.

In vivo study

Animal experiments were approved by the Animal Experimental Committee of Radboud University (RU-DEC-2019-0036). Luciferase-positive RCH-ACV p53^{KO} cells were intrafemorally engrafted in female NOD.Cg-Rag1tm1Mom Il2rgtm-1Wjl Tg (CMV-IL3,CSF2,KITLG)1Eav/J (NRG-SGM3, Jackson

Laboratory) mice. Starting 3 days after engraftment, mice were randomly assigned to groups of seven mice treated with either 17.5 mg/kg cytarabine (in double distilled H₂O; 5 days on, 2 days off), 1.5 mg/kg romidepsin (2% dimethylsulfoxide, 30% PEG 300, 5% Tween 80, 62% double distilled H₂O; every 1st and 4th day of the week), and/or placebo(s) for 21 days or until an endpoint was reached. Tumor load was monitored twice weekly via bioluminescence after intravenous injection of luciferin (D-luciferin, #ab143655, Abcam) and subsequent measurement of released photons using the IVIS Spectrum In Vivo Imaging System (Xenogen, now Perkin-Elmer).

Results

Loss of p53 functions confers resistance to most drugs used to treat B-cell precursor acute lymphocytic leukemia

Aberrations that affect the *TP53* gene are enriched in relapsed ALL and predict therapy failure, although how *TP53* affects responses to specific drugs used for relapsed ALL has not been explored. Therefore, we generated isogenic *TP53* wild-type/knockout pairs from the p53^{WT} BCP-ALL cell lines Nalm6 and RCH-ACV (Figure 1A). For initial validation, cells were treated with either the MDM2 inhibitor nutlin-3 (which prevents proteasomal degradation of p53 by inhibiting its ubiquitination) or the anthracycline daunorubicin. Both drugs induced elevated levels of p53, as well as the two key p53 effector proteins cyclin-dependent kinase inhibitor 1 (p21) and p53 upregulated modulator of apoptosis (PUMA), in p53-proficient cells (Figure 1A, B). In addition, apoptosis was induced in response to exposure to either drug, as determined by poly-ADP ribose polymerase (PARP) cleavage. In contrast, these effects were not observed in the p53^{KO} cells. Consistently, p53^{KO} models were significantly more resistant to drug-induced apoptosis than were their wild-type counterparts (Figure 1C, D). Having validated these models, we tested differential sensitivity to every drug currently used in the treatment of BCP-ALL. Both p53^{KO} cell lines showed increased resistance, relative to their p53^{WT} counterparts, to every drug tested (Figure 1E) and exhibited a clear survival advantage after drug treatment when combined in one culture (*Online Supplementary Figure S1A*). These experiments indicate that ALL cells lacking *TP53* are much less responsive to standard-of-care drugs used to treat BCP-ALL.

Romidepsin sensitizes B-cell precursor acute lymphocytic leukemia cells to therapy

To identify therapies that can potentially restore treatment response in *TP53*-deficient leukemia, we performed a high-throughput drug screen to determine the sensitivity of the p53^{WT} and p53^{KO} cells to a custom pediatric cancer drug library, comprising 198 standard-of-care drugs as

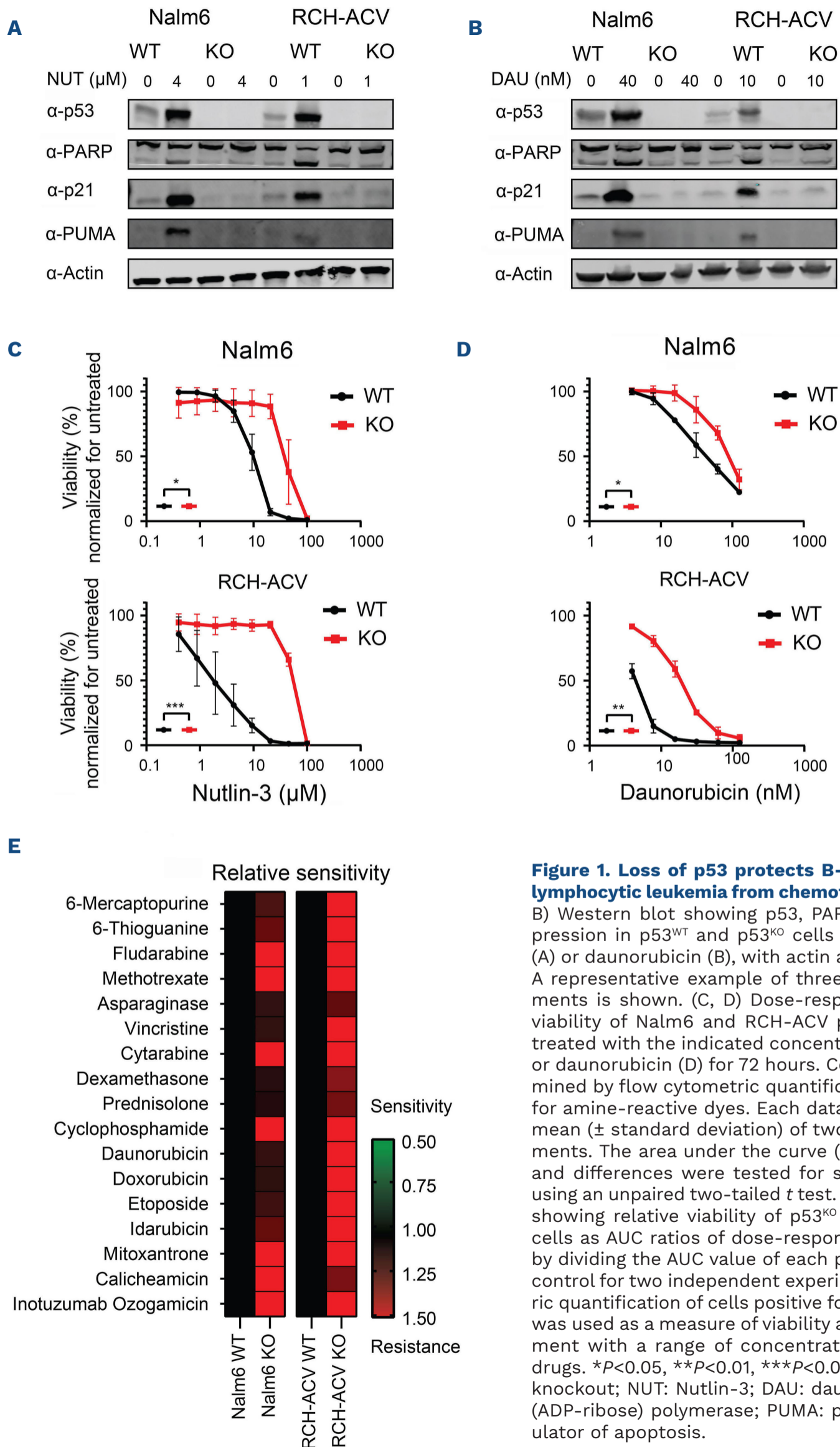


Figure 1. Loss of p53 protects B-cell precursor acute lymphocytic leukemia from chemotherapy treatment. (A, B) Western blot showing p53, PARP, p21 and PUMA expression in p53^{WT} and p53^{KO} cells treated with Nutlin-3 (A) or daunorubicin (B), with actin as the loading control. A representative example of three independent experiments is shown. (C, D) Dose-response curves showing viability of Nalm6 and RCH-ACV p53^{WT} and p53^{KO} cells treated with the indicated concentrations of Nutlin-3 (C) or daunorubicin (D) for 72 hours. Cell viability was determined by flow cytometric quantification of cells positive for amine-reactive dyes. Each data point represents the mean (± standard deviation) of two independent experiments. The area under the curve (AUC) was determined and differences were tested for statistical significance using an unpaired two-tailed *t* test. (E) Heatmap of results showing relative viability of p53^{KO} Nalm6 and RCH-ACV cells as AUC ratios of dose-response curves, calculated by dividing the AUC value of each p53^{KO} cell by the p53^{WT} control for two independent experiments. Flow cytometric quantification of cells positive for amine-reactive dyes was used as a measure of viability after 72 hours of treatment with a range of concentrations of the indicated drugs. **P*<0.05, ***P*<0.01, ****P*<0.001. WT: wild-type; KO: knockout; NUT: Nutlin-3; DAU: daunorubicin; PARP: poly (ADP-ribose) polymerase; PUMA: p53 upregulated modulator of apoptosis.

well as targeted compounds in early-phase clinical trials. Consistent with our earlier observations, p53^{KO} cells were resistant to MDM2 inhibitors such as idasanutlin, milademetan, and siremadlin as well as to nearly all included standard-of-care drugs (Figure 2A, extended results in *Online Supplementary Figure S1B*). Although we did not find any drug that selectively killed p53^{KO} cells, we did identify compounds that were effective against both wild-type and p53^{KO} cells. One of these compounds, the histone deacetylase (HDAC) 1/2 inhibitor romidepsin, effectively increased histone 3 acetylation and induced apoptosis in the low nanomolar range (*Online Supplementary Figure S2A-C*). While HDAC inhibitors frequently have little clinical activity as monotherapy, these compounds show promise when they are used to enhance conventional chemotherapy.¹⁰ We therefore tested whether romidepsin was able to potentiate the efficacy of cytarabine, an important drug in the current treatment protocols for relapsed/refractory ALL. We observed that romidepsin was able to fully restore therapy response in *TP53*-deficient ALL cells treated with cytarabine and enhanced response in *TP53*-proficient cells (Figure 2B, C). The observed synergy between cytarabine and romidepsin was recapitulated in all tested BCP-ALL cell lines, irrespective of their p53 status (*Online Supplementary Figure S2D*). Similarly, a combination of cytarabine with HDAC inhibitors tucidinostat and entinostat (inhibiting HDAC 1, 2, 3, and 10, and HDAC 1 and 3, respectively) produced comparable synergies (*Online Supplementary Figure S2E*), showing that this effect is not restricted to the specific chemical properties of romidepsin. However, as its effective concentration is up to 250 times lower than that of its tested peers, romidepsin was chosen to test the effects of HDAC inhibition on other drugs used to treat ALL. To confirm observations in cell lines, we tested the efficacy of combining romidepsin and cytarabine in 19 patient-derived xenografts (PDX), of which three p53 wildtype, six p53-aberrant (mutant and/or deleted), and ten with an undetermined p53 status (Figure 2D, viability curves in *Online Supplementary Figure S3*, p53 status in *Online Supplementary Table S2*). Regardless of p53 status, 17 PDX showed clear reductions in AUC values of viability when treated with both romidepsin and cytarabine compared to cytarabine alone. Moreover, the combination of romidepsin and cytarabine proved to be synergistic in ten of these 17 PDX. To expand the potential of romidepsin in combination with other drugs, we first combined it with inotuzumab ozogamicin, a recently introduced antibody-drug conjugate that is currently being used as a last-resort drug for high-risk relapsed BCP-ALL and confirmed the synergistic potential of this combination (Figure 2C, E). Finally, we combined romidepsin with all other therapy drugs and observed that romidepsin enhanced response to each of the tested drugs (Figure 3, full synergy landscapes in *Online Supplementary Figure S4*) sensitizing both p53^{KO} and p53^{WT} cells. Together, these results indicate that romidepsin

effectively improves the therapeutic efficacy of commonly used drugs regardless of p53 status, both in BCP-ALL cell lines and in patient-derived cells.

Romidepsin increases cytarabine-induced apoptosis by downregulation of components of the proteasome and ribosome biogenesis

Since histone acetylation induces global changes in gene expression, HDAC inhibition may act on many different pathways to affect response to therapy. To obtain further insights into these mechanisms, we performed bulk RNA sequencing on p53-deficient and p53-proficient cells treated with romidepsin, cytarabine, or their combination. We hypothesized that p53-deficient cells would show a reduced ability to induce p53 target genes and genes involved in the execution of apoptosis. Using GSEA with the MSigDB hallmark gene set collection⁷ (comprising 50 gene sets, including DNA damage and repair, apoptosis, glycolysis and p53 pathway gene sets) on the comparison of cytarabine-treated wild-type cells *versus* knockout cells, we confirmed enrichment of both p53 target genes and apoptosis-related genes in p53-proficient cells compared to p53-deficient cells (*Online Supplementary Figure S5A*). We confirmed by quantitative real-time polymerase chain reaction (qRT-PCR) analysis that induction of the p53 target genes *CDKN1A* (protein: p21), *BBC3* (PUMA), and *GADD45A* (GADD45a) was compromised in p53-deficient cells (*Online Supplementary Figure S5B*), while differences in apoptosis induction were already established (Figure 2C). *PMAIP1* (NOXA) induction was not affected by p53 loss, consistent with the notion that this gene, apart from being a p53 target, can mediate apoptosis in a p53-independent manner in hematologic malignancies.¹¹

To test whether romidepsin may act to (re)activate p53 target genes and thereby induce apoptosis, we performed GSEA, again using the MSigDB hallmark gene set collection which includes gene sets that cover p53 pathway or apoptosis, comparing both romidepsin-only *versus* control treatment and combination *versus* cytarabine-only treatment (normalized enrichment scores, *P* values and false discovery rate *q* values of HALLMARK_APOPTOSIS and HALLMARK_P53_PATHWAY are shown in *Online Supplementary Table S3*). We found significantly enhanced apoptosis in three out of four models for both comparisons (non-significant enrichment of RCH-ACV wild-type for romidepsin *versus* control, normalized enrichment score 1.23, *P*=0.133; and Nalm6 wild-type near significant in combination *versus* cytarabine, normalized enrichment score 1.31, *P*=0.06). However, we did not observe a consistently significant enrichment of the p53 pathway across our models when comparing either romidepsin-only to control treatment, or combination treatment to cytarabine-only (*Online Supplementary Table S3*). Thus, while romidepsin does induce apoptosis, this does not appear to require p53.

To identify other mechanisms of action of romidepsin,

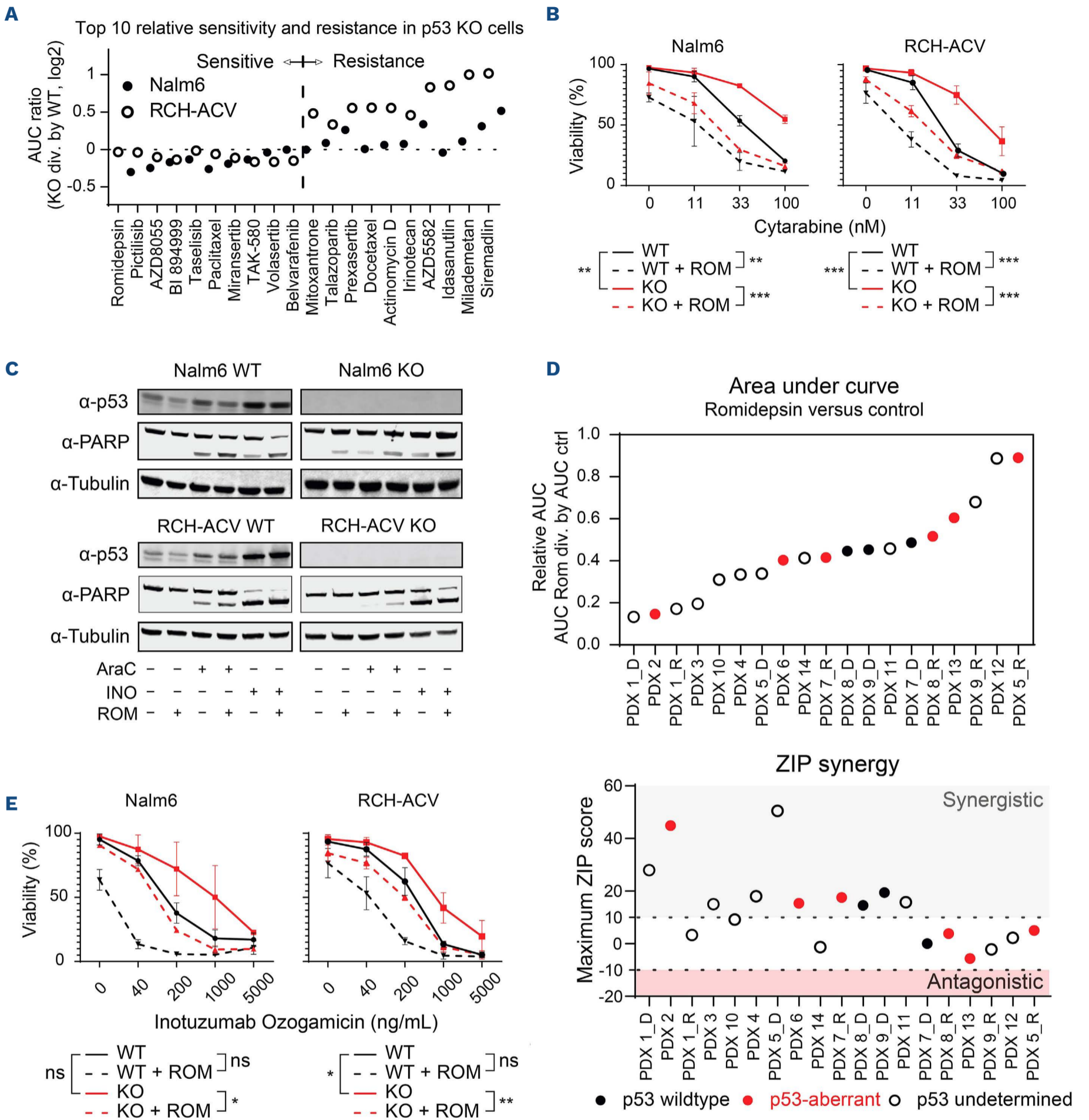


Figure 2. Romidepsin sensitizes p53-deficient and p53-proficient cells to cytarabine and inotuzumab. (A) Results of the drug screen showing the relative viability of p53^{KO} Nalm6 and RCH-ACV cells as area under the curve (AUC) ratios, calculated by dividing the AUC value of each p53^{KO} cell by that of the p53^{WT} control. 3-(4,5-dimethylthiazol-2-yl)-2,5-diphenyltetrazolium bromide (MTT) conversion was used as a measure of viability after treatment with a range of concentrations of the indicated drug for 72 hours (n=1). (B) Dose-response curves showing viability of Nalm6 and RCH-ACV p53^{WT} and p53^{KO} cells treated with the indicated concentrations of cytarabine in the presence or absence of romidepsin (2.25 nM) for 72 hours as determined by flow cytometric quantification of cells positive for amine-reactive dyes. Each data point represents the mean (± standard deviation [SD]) of two independent experiments. The AUC was determined and differences were tested for statistical significance using analysis of variance (ANOVA) followed by Tukey multiple comparisons tests. (C) Western blot showing p53 and PARP expression in p53^{WT} and

Continued on following page.

p53^{KO} cells treated with romidepsin (2 nM), cytarabine (30 nM), and/or inotuzumab ozogamicin (Nalm6, 200 ng/mL; RCH-ACV, 100 ng/mL) for 24 hours, with tubulin as the loading control. A representative example of three independent experiments is shown. (D) Fourteen patient-derived xenograft (PDX) samples from subjects with B-cell precursor acute lymphoblastic leukemia were seeded on hTERT-immortalized mesenchymal stromal cells and treated with the indicated concentrations of romidepsin and/or cytarabine for 72 hours. Flow cytometric quantification of cells positive for amine-reactive dyes was used as a measure of viability and as an input for AUC and zero interaction potency (ZIP) synergy calculations. AUC ratios were calculated by dividing the AUC value of the dose-response curve of the combination of romidepsin (2 or 2.25 nM, depending on the PDX) and a range of cytarabine concentrations by that of the cytarabine-only curve. Maximum ZIP synergy scores were computed from the viability response after romidepsin (at a concentration ranging from 0.5–8 nM) and/or cytarabine treatment (at a concentration ranging from 0.1 nM–100 μ M). Diagnosis-relapse pairs of samples from the same patient are indicated by suffixes _D and _R. Data shown are n=1 for each PDX. (E) Dose-response curves showing viability of Nalm6 and RCH-ACV p53^{WT} and p53^{KO} cells treated with the indicated concentrations of inotuzumab ozogamicin in the presence or absence of romidepsin (2.25 nM) for 72 hours as determined by flow cytometric quantification of cells positive for amine-reactive dyes. Each data point represents the mean (\pm SD) of two independent experiments. The AUC was determined and differences were tested for statistical significance using ANOVA followed by Tukey multiple comparisons tests. ns: not statistically significant, * P <0.05, ** P <0.01, *** P <0.001. KO: knockout; WT: wild-type; ROM: romidepsin; PARP: poly (ADP-ribose) polymerase; AraC: cytarabine; INO; inotuzumab ozogamicin; PDX: patient-derived xenograft; ZIP: zero interaction potency.

we performed differential gene expression calculations for every possible treatment combination per cell model, filtered for significance (P <0.05) and fold change (\log_2 fold change smaller than -0.5 or greater than 0.5), calculated z-scores per filtered gene for both genotypes per cell line and generated heatmaps (Nalm6 p53^{KO} shown in Figure 4A, remaining models in *Online Supplementary Figure S6A*). These heatmaps showed clusters of genes that are either upregulated or downregulated in both romidepsin-only versus control and combination versus cytarabine-only comparisons (as indicated in Figure 4A and *Online Supplementary Figure S6A*). Only a small number of genes (21 genes) was consistently activated in all four cell models (Figure 4B), and pathway analysis of these genes did not lead to significant pathway correlation. In contrast, gene suppression as a result of romidepsin treatment was a more general effect, with 237 downregulated genes shared by all models (Figure 4B), and subsequent Kyoto Encyclopedia of Genes and Genomes (KEGG) pathway analysis revealed significant enrichment for genes involved in ribosome biogenesis and proteasome assembly (Figure 4C). We again validated this downregulation with qRT-PCR, assessing the mRNA expression of four genes per pathway included in the downregulated clusters (*Online Supplementary Figure S6B, C*). To assess whether the downregulation of these pathways renders cells more sensitive to chemotherapy, we combined inhibitors of the proteasome (carfilzomib and bortezomib) or ribosome biogenesis (actinomycin D) with cytarabine (Figure 5). Indeed, both proteasome inhibition and ribosome biogenesis perturbation showed synergy with cytarabine, albeit with lower synergy values compared to those with romidepsin, suggesting that neither one of these effects fully recapitulates the effects of romidepsin in enhancing therapy-induced apoptosis (*Online Supplementary Figure S6D*). We conclude from these results that romidepsin treatment leads to the downregulation of components of ribosome biogenesis and the proteasome and that this may, at least in part, contribute to an increased sensitivity to cytarabine.

Romidepsin improves the response to cytarabine *in vivo*

We next tested whether the combination of cytarabine and romidepsin would be effective *in vivo*. In order to do this, immunocompromised mice were transplanted with luciferase-expressing RCH-ACV p53^{KO} cells. Three days after trans-

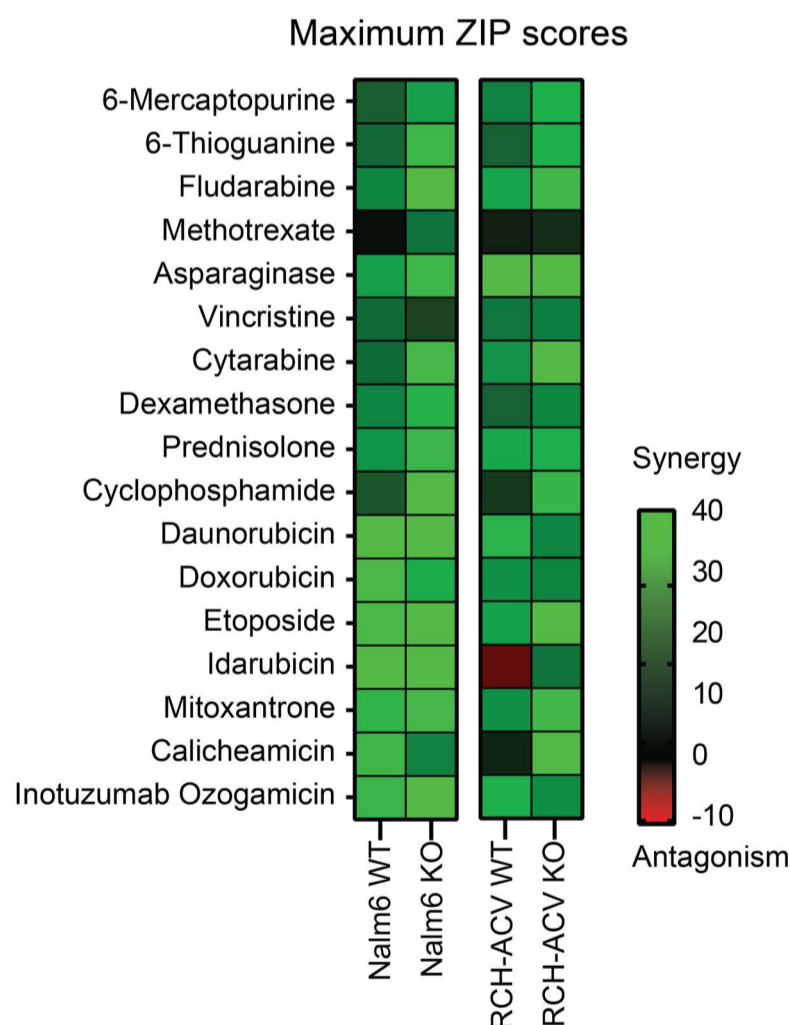


Figure 3. Romidepsin sensitizes p53-deficient and p53-proficient cells to therapy for B-cell precursor acute lymphocytic leukemia therapy *in vitro*. Heatmap of maximum zero interaction potency synergy scores for two independent experiments. Nalm6 and RCH-ACV p53^{KO} cells were exposed to five concentrations of romidepsin (0–3.375 nM) and five concentrations of the drug listed per row for 72 hours. Flow cytometric quantification of cells positive for amine-reactive dyes was used as a measure of viability and as input for synergy calculations. ZIP: zero interaction potency; WT: wild-type; KO: knockout.

plantation, the mice were treated with vehicle, cytarabine, romidepsin, or a combination of both drugs (Figure 6A). This treatment regimen was well tolerated as evidenced by a constant body weight during treatment (*Online Supplementary Figure S7*). Leukemia burden was assessed during and after treatment by measurement of photon flux following lucifer-

in injection. Mice treated with romidepsin as a single agent did not benefit from treatment, whereas a short course of treatment with cytarabine was sufficient to delay leukemia development (Figure 6B, C). Importantly, in mice treated with the combination regimen, leukemia development was significantly delayed compared to that in the animals treated

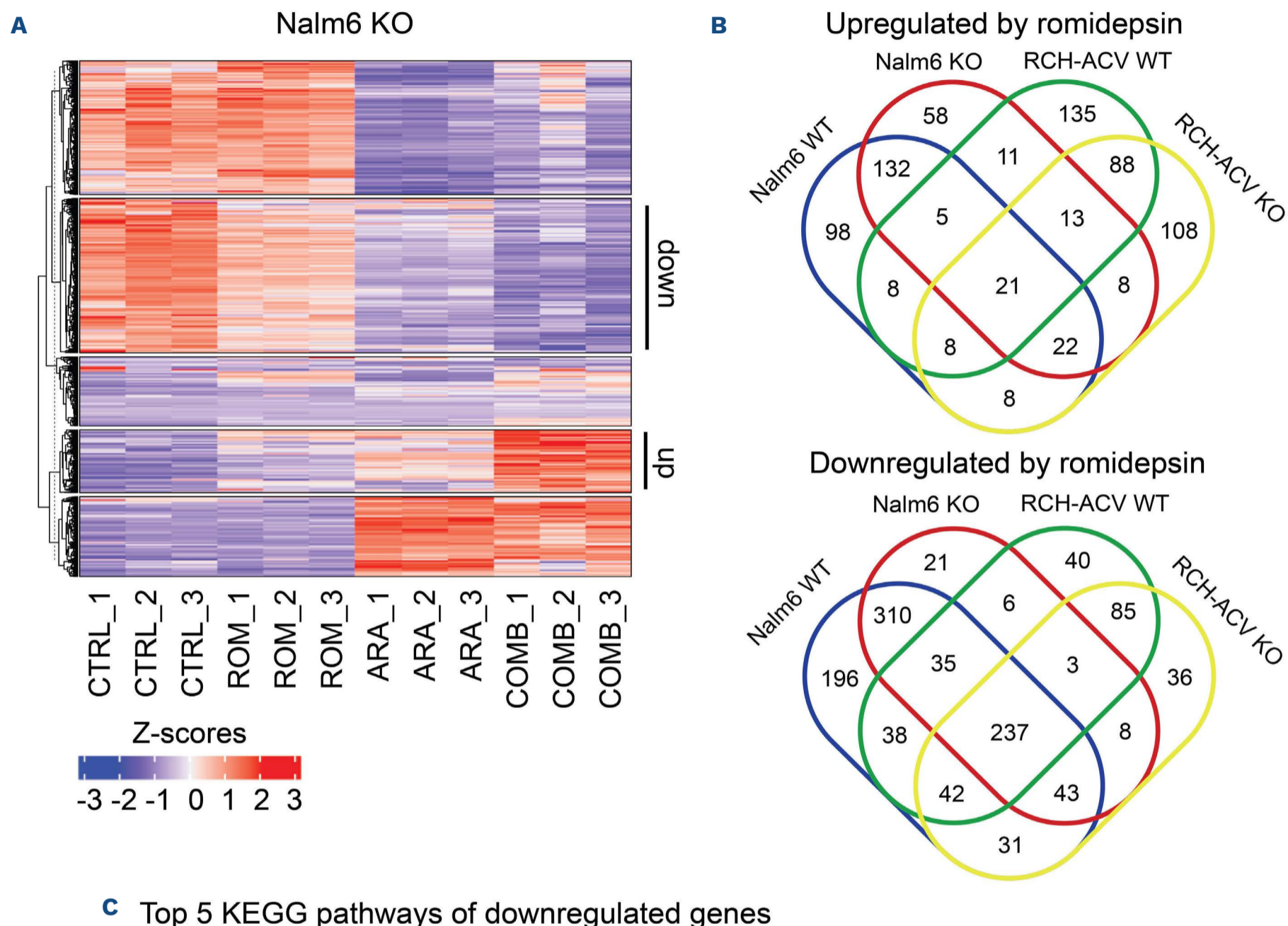


Figure 4. RNA sequencing reveals transcriptional effects of cytarabine and romidepsin treatment. (A) Heat map showing gene-expression levels from RNA-sequencing analysis in Nalm6 p53^{KO} cells treated with cytarabine and/or romidepsin. Calculations of differentially expressed genes were performed for every possible treatment combination within a cell line and filtered for genes with a *P* value of less than 0.05 and a log₂ cutoff of smaller than -0.5 or greater than 0.5. Gene lists were then combined for both genotypes per cell line, Z scores were computed and heatmaps were generated for each model in RStudio using unsupervised clustering. Clusters of up- (up) and downregulated (down) genes in both the comparisons of romidepsin *versus* control treatment and combination *versus* cytarabine treatment are indicated. (B) Venn diagram of overlapping differentially expressed gene lists either consistently upregulated (top) or downregulated (bottom) upon romidepsin treatment in the four tested models. (C) The top five Kyoto Encyclopedia of Genes and Genomes (KEGG) pathways associated with the shared genes are depicted in the bottom panel of (B) according to the Search Tool for the Retrieval of Interacting Genes/Proteins (STRING) algorithm. KO: knockout; CTRL: control; ROM: romidepsin; ARA: cytarabine; COMB: combination therapy; WT: wild-type; FDR: false discovery rate.

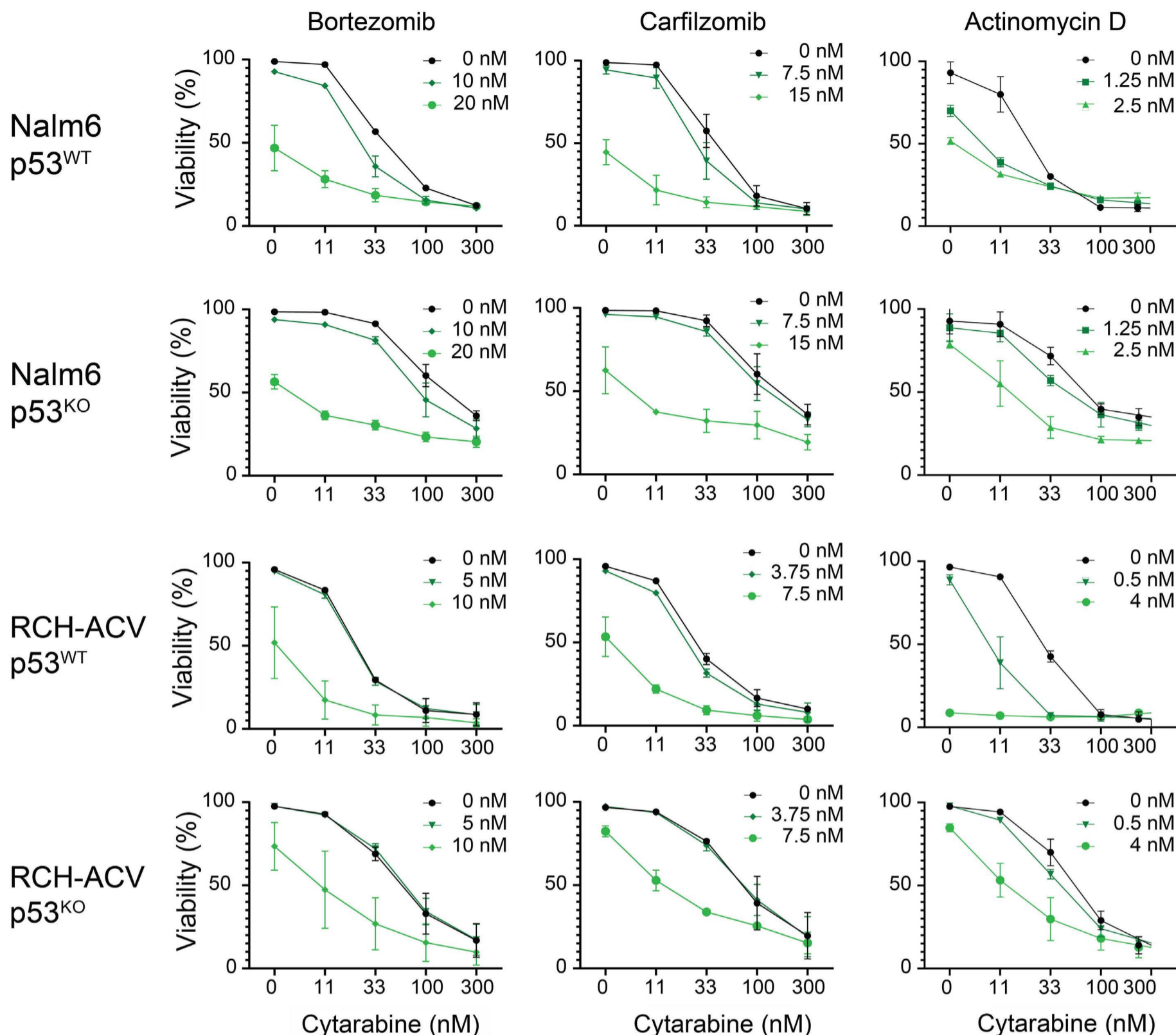


Figure 5. Inhibition of ribosome biogenesis or the proteasome sensitizes B-cell precursor acute lymphocytic leukemia cells to cytarabine *in vitro*. Dose-response curves showing the viability of Nalm6 and RCH-ACV p53^{WT} and p53^{KO} cells treated with the indicated concentrations of cytarabine in the presence or absence of the proteasome inhibitors bortezomib and carfilzomib, and the ribosome biogenesis inhibitor actinomycin D for 72 hours as determined by flow cytometric quantification of cells positive for amine-reactive dyes. Each data point represents the mean (\pm standard deviation) of two independent experiments. WT: wild-type; KO: knockout.

with cytarabine only, showing that romidepsin synergizes with cytarabine *in vivo* without causing any overt signs of toxicity. We conclude from these results that romidepsin may potentially be used to enhance response to therapy in relapsed/refractory TP53-deficient leukemias.

Discussion

The treatment of relapsed BCP-ALL involves high-dose chemotherapeutics that may be followed by hematopoi-

etic stem cell transplantation. Ongoing clinical trials are studying the potential benefit of various immunotherapies, including antibody-drug conjugates, T-cell engagers, and chimeric antigen receptor (CAR) T-cell therapy. Loss of p53 functions predicts a dismal outcome in relapsed BCP-ALL that is treated with conventional protocols and initial observations indicate a poor response to CAR T-cell therapy.¹² Similarly, the efficacy of inotuzumab ozogamicin, an antibody-drug conjugate that is highly effective for the treatment of relapsed B-cell ALL, is impaired in TP53-mutated leukemia as reported by Tirrò *et al.*¹³ and shown in

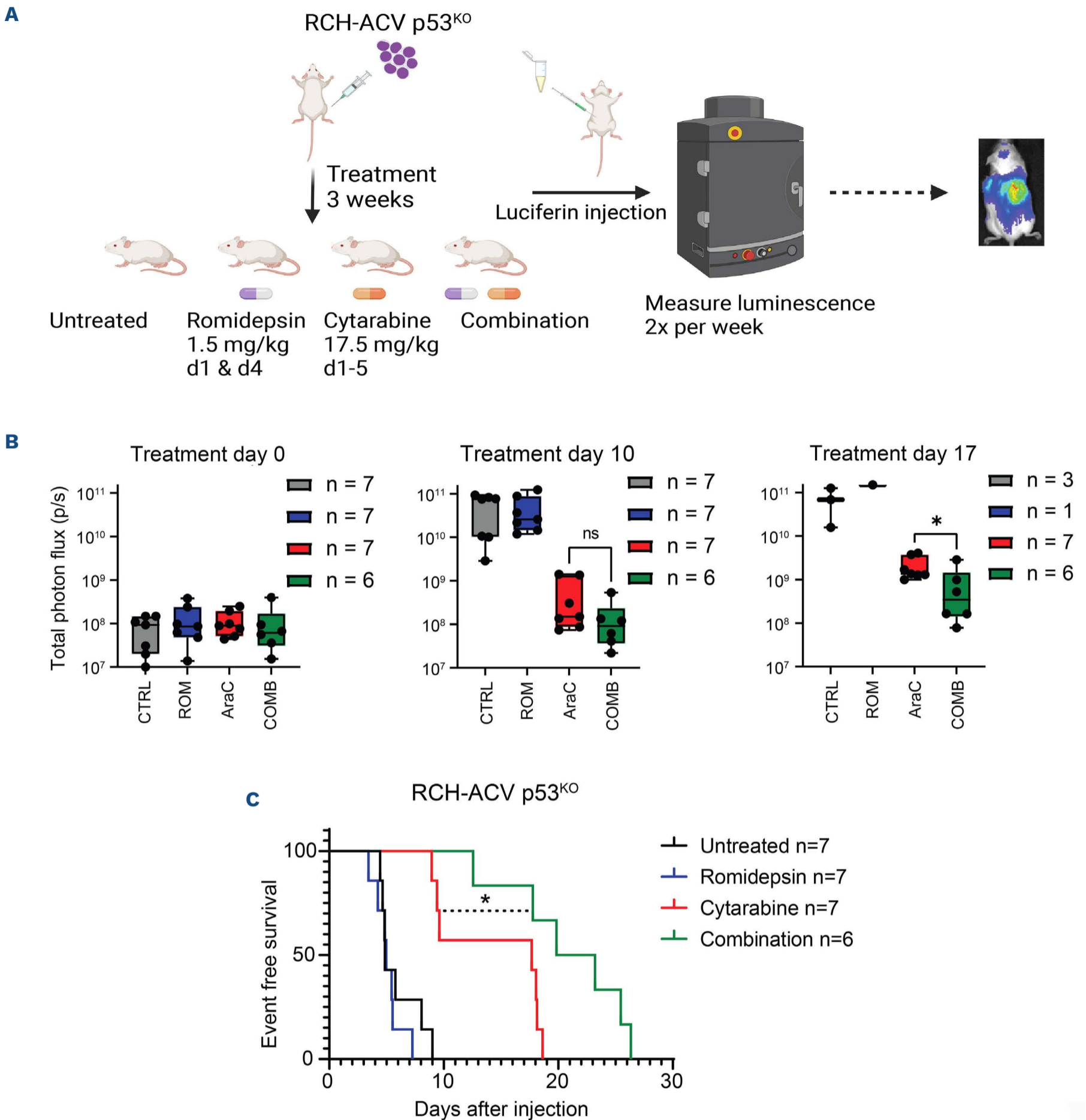


Figure 6. Romidepsin sensitizes p53-deficient cells to cytarabine *in vivo*. (A) Schematic representation of the setup of the *in vivo* experiment. Luciferase-expressing RCH-ACV p53^{KO} cells were injected into NRG-SM3 mice and treated for 3 weeks with cytarabine, romidepsin, or their combination. Leukemia development was followed by measuring luciferase-induced photon flux. Image created with BioRender.com. (B) Total photon flux is visualized for the start of treatment and days 10 and 17 of treatment. Differences were tested for statistical significance using a Mann-Whitney test comparing the cytarabine and combination groups as data in these groups were not normally distributed. (C) Kaplan-Meier plot of NRG-SM3 mice transplanted with luciferase-expressing RCH-ACV p53^{KO} cells under treatment with cytarabine, romidepsin or their combination. An event was defined as a tumor load reaching a total photon flux of 5×10^8 photons per second. Differences were tested using a log-rank test comparing the cytarabine and combination groups. ns: not significant; * $P < 0.05$. KO: knockout; CTRL: control; ROM: romidepsin; AraC: cytarabine; COMB: combination therapy; WT: wild-type.

Figure 2C, E. Hence, despite the advances that are being made for other subtypes of relapsed BCP-ALL, there is an urgent clinical need for the development of novel therapeutic strategies that effectively eradicate *TP53*-mutated leukemia.

In the past few decades, drugs that modulate the epigenome, including hypomethylating agents and HDAC inhibitors have shown promise in anti-cancer treatment.^{14,15} In hematologic malignancies, in particular, oncogenic driver mutations are commonly found in genes involved in epigenetic modifications, suggesting that these tumors may be sensitive to drugs targeting epigenetic regulators. While the clinical efficacy of these drugs as monotherapy is limited, the combination of a hypomethylating agent and a Bcl-2 inhibitor was shown to be highly effective in the treatment of patients with acute myeloid leukemia who are unfit for curative chemotherapy-based protocols.^{16,17}

Altogether, our results indicate that loss of p53 function renders BCP-ALL cells resistant to most currently used (chemo)therapies, but that HDAC inhibition by romidepsin can resensitize these cells to therapy. In contrast to earlier findings by Yan *et al.*¹⁸ in acute myeloid leukemia, we did not observe specific transcriptional (re)activation of the p53 pathway upon romidepsin treatment in p53-deficient cells, which may be explained by the different cellular context that was tested. The transcriptome data and validations presented here instead suggest that inhibition of ribosome biogenesis and the proteasome, both associated with apoptosis given the appropriate context, may be involved in the increased apoptotic response observed when cytarabine treatment is combined with romidepsin. Potential mechanisms through which class I histone deacetylases such as HDAC1 and HDAC2, the main targets of romidepsin, can affect gene expression may include regulating histone acetylation and thereby chromatin accessibility,¹⁹ as well as allowing the formation of a complex with corepressors such as NCoR or SMRT which may lead to gene repression.²⁰⁻²² The latter has been implicated in differentiation of acute myeloid leukemia, most notably in the context of the fusion genes *PML-RAR* and *AML1-ETO*.²³ Of note, both Nalm6 (*IGH-DUX4*) and RCH-ACV (*TCF3-PBX1*) carry gene fusions. However, it remains to be seen to what extent such mechanisms may contribute to the observed synergy involving HDAC inhibition in BCP-ALL.

Consistent with our findings that romidepsin improves response to therapy regardless of p53 status, romidepsin was previously found to improve response to therapy in *KMT2A*-rearranged leukemia.^{24,25} It appears that romidepsin is effective in both p53-deficient as well as some p53-proficient subsets of ALL and may therefore represent a valuable addition to the current treatment protocols for (relapsed) BCP-ALL. As the effects on the proteasome seem to contribute to the observed synergy of romidepsin, it is

important to note that the proteasome inhibitor bortezomib has previously been added to a chemotherapy backbone in relapsed pediatric B-ALL and T-ALL patients, demonstrating manageable toxicity and clinical efficacy.²⁶⁻²⁹ However, our results show that proteasome inhibition alone does not fully recapitulate the synergy observed with romidepsin, and therefore romidepsin may be even more effective in improving therapy response on a (chemo)therapy backbone. Clinically, romidepsin was previously tested as a single agent in both adults and children, showing manageable toxicities.^{30,31} More recently, romidepsin was combined with doxorubicin as well as the immunomodulatory agent lenalidomide in phase I or II trials, showing clinical efficacy and feasibility in the treatment of hematologic malignancies.^{32,33} Together, these results highlight a potential for romidepsin combination regimens in hematologic malignancies. Further (pre)clinical studies should reveal whether romidepsin may be used to improve current or experimental salvage therapies for relapsed *TP53*-deficient ALL.

Disclosures

No conflicts of interest to disclose.

Contributions

FNvL, LTvdM, MB, and WPJC conceptualized the project. FNvL and LTvdM supervised the work. WPJC performed the experiments with assistance from NE, DSvIS, GRS, NA, LdG, and MB. KJTG, RH, and RPK contributed to analyzing the data. RPK assisted with genotyping samples. DSvIS generated the xenografts. WPJC, LTvdM, and FNvL drafted the manuscript which was reviewed, and approved by all the authors.

Acknowledgments

The authors thank members of the flow cytometry facility, the high throughput screening facility (<https://research.prinsesmaximacentrum.nl/en/core-facilities/high-throughput-screening>) and the Kuiper research group in the Princess Máxima Center, and the PRIME department of RadboudUMC animal facility for valuable technical support. In addition, the authors thank MRC Holland for providing digital MLPA data and Vaskar Saha for providing the pLNT-Sffv-luciferase plasmid. pSpCas9(BB)-2A-GFP was a gift from Feng Zhang (Addgene plasmid # 48138; RRID: Addgene_48138).

Funding

This work was supported by the Princess Máxima Center for Pediatric Oncology.

Data-sharing statement

The data generated in this study are available within the article and its supplementary data files. Transcriptome data generated in the study are publicly available in Gene Expression Omnibus (GEO) (GSE234091).

References

- Inaba H, Mullighan CG. Pediatric acute lymphoblastic leukemia. *Haematologica*. 2020;105(11):2524-2539.
- Donehower LA, Soussi T, Korkut A, et al. Integrated analysis of TP53 gene and pathway alterations in The Cancer Genome Atlas. *Cell Rep*. 2019;28(5):1370-1384.
- Hof J, Krentz S, Van Schewick C, et al. Mutations and deletions of the TP53 gene predict nonresponse to treatment and poor outcome in first relapse of childhood acute lymphoblastic leukemia. *J Clin Oncol*. 2011;29(23):3185-3193.
- Kanagal-Shamanna R, Kantarjian HM, Khoury JD, et al. Distinct prognostic effects of TP53 mutations in newly diagnosed versus relapsed/refractory (R-R) patients (pts) with B-acute lymphoblastic leukemia (ALL) treated with mini-Hcvt- inotuzumab ozogamicin with or without blinatumomab regimens. *Blood*. 2020;136(Suppl 1):41-43.
- Kastenhuber ER, Lowe SW. Putting p53 in context. *Cell*. 2017;170(6):1062-1078.
- Frismantas V, Dobay MP, Rinaldi A, et al. Ex vivo drug response profiling detects recurrent sensitivity patterns in drug-resistant acute lymphoblastic leukemia. *Blood*. 2017;129(11):26-37.
- Liberzon A, Birger C, Thorvaldsdóttir H, Ghandi M, Mesirov JP, Tamayo P. The Molecular Signatures Database (MSigDB) hallmark gene set collection. *Cell Syst*. 2015;1(6):417-425.
- Mootha VK, Lindgren CM, Eriksson K-F, et al. PGC-1 α -responsive genes involved in oxidative phosphorylation are coordinately downregulated in human diabetes. *Nat Genet*. 2003;34(3):267-273.
- Subramanian A, Tamayo P, Mootha VK, et al. Gene set enrichment analysis: a knowledge-based approach for interpreting genome-wide expression profiles. *Proc Natl Acad Sci U S A*. 2005;102(43):15545-15550.
- Hontecillas-Prieto L, Flores-Campos R, Silver A, de Álava E, Hajji N, García-Domínguez DJ. Synergistic enhancement of cancer therapy using HDAC inhibitors: opportunity for clinical trials. *Front Genet*. 2020;11:578011.
- Fidyk K, Pastorczak A, Cyran J, et al. Potent, p53-independent induction of NOXA sensitizes MLL-rearranged B-cell acute lymphoblastic leukemia cells to venetoclax. *Oncogene*. 2022;41(11):1600-1609.
- Zhang X, Lu X-A, Yang J, et al. Efficacy and safety of anti-CD19 CAR T-cell therapy in 110 patients with B-cell acute lymphoblastic leukemia with high-risk features. *Blood Adv*. 2020;4(10):2325-2338.
- Tirró E, Massimino M, Romano C, et al. Chk1 inhibition restores inotuzumab ozogamicin cytotoxicity in CD22-positive cells expressing mutant p53. *Front Oncol*. 2019;9:57.
- Bennett RL, Licht JD. Targeting epigenetics in cancer. *Annu Rev Pharmacol Toxicol*. 2018;58(1):187-207.
- Ho TCS, Chan AHY, Ganesan A. Thirty years of HDAC inhibitors: 2020 insight and hindsight. *J Med Chem*. 2020;63(21):12460-12484.
- San José-Enériz E, Gimenez-Camino N, Agirre X, Prosper F. HDAC Inhibitors in acute myeloid leukemia. *Cancers (Basel)*. 2019;11(11):1794.
- DiNardo CD, Jonas BA, Pullarkat V, et al. Azacitidine and venetoclax in previously untreated acute myeloid leukemia. *N Engl J Med*. 2020;383(7):617-629.
- Yan B, Chen Q, Xu J, Li W, Xu B, Qiu Y. Low-frequency TP53 hotspot mutation contributes to chemoresistance through clonal expansion in acute myeloid leukemia. *Leukemia*. 2020;34(7):1816-1827.
- Gallinari P, Marco SD, Jones P, Pallaoro M, Steinkühler C. HDACs, histone deacetylation and gene transcription: from molecular biology to cancer therapeutics. *Cell Res*. 2007;17(3):195-211.
- Heinzel T, Lavinsky RM, Mullen T-M, et al. A complex containing N-CoR, mSin3 and histone deacetylase mediates transcriptional repression. *Nature*. 1997;387(6628):43-48.
- Wen Y-D, Perissi V, Staszewski LM, et al. The histone deacetylase-3 complex contains nuclear receptor corepressors. *Proc Natl Acad Sci U S A*. 2000;97(13):7202-7207.
- Alland L, Muhle R, Hou H Jr, et al. Role for N-CoR and histone deacetylase in Sin3-mediated transcriptional repression. *Nature*. 1997;387(6628):49-55.
- Minucci S, Nervi C, Lo Coco F, Pelicci PG. Histone deacetylases: a common molecular target for differentiation treatment of acute myeloid leukemias? *Oncogene*. 2001;20(24):3110-3115.
- Cruickshank MN, Ford J, Cheung LC, et al. Systematic chemical and molecular profiling of MLL-rearranged infant acute lymphoblastic leukemia reveals efficacy of romidepsin. *Leukemia*. 2017;31(1):40-50.
- Cheung LC, Cruickshank MN, Hughes AM, et al. Romidepsin enhances the efficacy of cytarabine in vivo, revealing histone deacetylase inhibition as a promising therapeutic strategy for KMT2A-rearranged infant acute lymphoblastic leukemia. *Haematologica*. 2019;104(7):300-303.
- Horton TM, Whitlock JA, Lu X, et al. Bortezomib reinduction chemotherapy in high-risk ALL in first relapse: a report from the Children's Oncology Group. *Br J Haematol*. 2019;186(2):274-285.
- Wang R, Wang W, Liu X, et al. Treatment for a B-cell acute lymphoblastic leukemia patient carrying a rare TP53 c.C275T mutation: a case report. *Front Oncol*. 2022;12:1018250.
- Miyagawa N, Goto H, Ogawa A, et al. Phase 2 study of combination chemotherapy with bortezomib in children with relapsed and refractory acute lymphoblastic leukemia. *Int J Hematol*. 2023;118(2):267-276.
- Teachey DT, Devidas M, Wood BL, et al. Children's Oncology Group trial AALL1231: a phase III clinical trial testing bortezomib in newly diagnosed T-cell acute lymphoblastic leukemia and lymphoma. *J Clin Oncol*. 2022;40(19):2106-2118.
- Fouladi M, Furman WL, Chin T, et al. Phase I study of depsipeptide in pediatric patients with refractory solid tumors: a Children's Oncology Group report. *J Clin Oncol*. 2006;24(22):3678-3685.
- Whittaker SJ, Demierre MF, Kim EJ, et al. Final results from a multicenter, international, pivotal study of romidepsin in refractory cutaneous T-cell lymphoma. *J Clin Oncol*. 2010;28(29):4485-4491.
- Ruan J, Zain J, Palmer B, et al. Multicenter phase 2 study of romidepsin plus lenalidomide for previously untreated peripheral T-cell lymphoma. *Blood Adv*. 2023;7(19):5771-5779.
- Vu K, Wu CH, Yang CY, et al. Romidepsin plus liposomal doxorubicin is safe and effective in patients with relapsed or refractory T-cell lymphoma: results of a phase I dose-escalation study. *Clin Cancer Res*. 2020;26(5):1000-1008.